

# Photosynthetic Electron Transport and Superoxide Dismutase Activity during Natural Senescence of Maple Leaves

Hrvoje Lepeduš,<sup>a,\*</sup> Ivna Štolfa,<sup>a</sup> Sandra Radić,<sup>b</sup> Mirna Ćurković Perica,<sup>b</sup>  
Branka Pevalek-Kozlina,<sup>b</sup> and Vera Cesar<sup>a</sup>

<sup>a</sup>Department of Biology, Josip Juraj Strossmayer University of Osijek, Trg Ljudevita Gaja 6, HR-31000 Osijek, Croatia

<sup>b</sup>Department of Botany, Faculty of Science, University of Zagreb, Rooseveltov trg 6, HR-10000 Zagreb, Croatia

RECEIVED MARCH 20, 2007; REVISED JULY 11, 2007; ACCEPTED JULY 18, 2007

*Keywords*  
senescence  
photosystem II  
Rubisco LSU  
SOD  
lipid peroxidation  
protein oxidation

Natural senescence of maple (*Acer pseudoplatanus* L.) leaves was investigated. Three types of senescing leaves were used: green (G), yellow-green (YG) and yellow (Y) ones. Down regulation of photosynthetic performance was achieved due to significant degradation of total chlorophylls, decrease in maximum quantum yield of PSII ( $F_v/F_m$ ) and relative electron transport rate (rel. ETR). Also, decrease in Rubisco LSU abundance as well as degradation of *rbcL* gene was shown in YG and Y leaves. Senescent leaves revealed significant increase in the capacity of PSII for oxygen evolution when expressed per chlorophyll unit. This was the most probable source of reactive oxygen species (ROS) excess. The level of SOD (superoxide dismutase) activity increased 3.5-fold in Y leaves in respect to G and YG leaves. The increase in ROS level as well as in SOD activity during natural senescence of maple leaves was associated with increased level of lipid peroxidation and protein carbonyl content.

## INTRODUCTION

Natural senescence of plant organs represents a developmentally regulated process.<sup>1</sup> It involves induction of senescence-associated genes (SAG) that, among others, encode degradative enzymes. Consequently ordered degradation of cell structures and organelles arises, leading to programmed cell death (PCD). A variety of internal and external stimuli were recognized as inducers of senescence. Since chloroplasts are known to be the primary sites of senescence process,<sup>2</sup> it is usual to follow the senescence in terms of chlorophyll degradation. Also, chloroplasts contain up to 70 % of all leaf proteins, predominantly Rubisco, what makes them the main source of ni-

trogen in leaves. Ordered dismantling of chloroplasts is therefore prerequisite for nutrient remobilization into younger parts of plant. Degradation of chloroplast components especially pigments and proteins impair photosynthetic performance which leads to increase in reactive oxygen species (ROS) production.<sup>3</sup> ROS have a dual role in the cell.<sup>4</sup> They can react with proteins, lipids, pigments, nucleic acids and other cellular components causing their degradation and dysfunction. Also, they have a role in cell signaling processes, which makes them possible candidates in regulation of senescence. Essential signaling processes such as changes in calcium mobilization, protein phosphorylation and gene expression are known to be modulated by H<sub>2</sub>O<sub>2</sub>.<sup>5</sup> Hence, the homeostasis in ROS

\* Author to whom correspondence should be addressed. (E-mail: [hlepedus@yahoo.com](mailto:hlepedus@yahoo.com))

abundance must be kept by diverse molecular mechanisms inside different cell compartments in order to assure avoidance of uncontrolled cell damage on the one side and the induction of ordered degradation of organelles, cell structures and biomolecules during senescence on the other one. Plants have developed very efficient systems to scavenge ROS.<sup>6</sup> Superoxide dismutases (SODs) are considered to be the first line of defense against oxidative damage caused by ROS.<sup>7</sup> SODs are metallo-enzymes that catalyze dismutation of superoxide radical ( $O_2^{\cdot -}$ ) to molecular oxygen and  $H_2O_2$ .<sup>8</sup> Since about 25 % of non cyclic electron transport in chloroplasts can be attributed to Mehler reaction,<sup>7</sup> which produces superoxide, it is very important to remove excess superoxide as well as to prevent formation of very destructive hydroxyl ( $OH^{\cdot}$ ) and hydroperoxyl radicals ( $HO_2^{\cdot}$ ). Besides superoxide radicals, the over-reduction of electron-transport chain in chloroplasts leads to the formation of highly toxic singlet oxygen ( $^1O_2$ ) which reacts with most organic molecules.<sup>8,9</sup>

Although the leaf senescence and PCD were extensively explored at different levels of plant organization and functioning,<sup>10</sup> most data obtained originate from experiments with herbaceous species or from experimentally induced senescence. However, much less is known about regulatory mechanisms of natural leaf senescence in woody species. The objective of this study was to investigate modulation of photosynthetic electron transport and superoxide dismutase (SOD) activity during maple (*Acer pseudoplatanus* L.) leaf yellowing in correlation with oxidative damage to lipids and proteins.

## EXPERIMENTAL

### Plant Material

Three different types of senescing maple (*Acer pseudoplatanus* L.) leaves: green (G), yellow green (YG) and yellow (Y) were harvested in October 2005 from three different trees. The combined sample was made for each leaf type and five replicates were taken for every analysis. In all determinations leaf tissue was used after the main veins were removed.

### Photosynthetic Parameters

The leaf tissue was macerated into fine powder with liquid nitrogen using pestle and mortar. Approximately 0.15 g of this fine tissue powder was extracted with 1 ml of the cold anhydrous acetone ( $\rho = 0.79 \text{ kg dm}^{-3}$ ). The material was re-extracted about four times until it was completely uncolored. Quantitative determination of total chlorophylls (Chl *a+b*) was done by measuring the absorbance at different wavelengths (661.6 and 644.8 nm) using an Analytik Jena Specord 40 spectrophotometer. The concentrations of total chlorophylls were calculated according to Lichtenthaler.<sup>11</sup>

Relative photosynthetic electron transport rate (rel. ETR) was determined by measuring chlorophyll *a* fluorescence *in vivo* using a pulse amplitude modulated fluorometer

(miniPAM, Walz). Leaves were kept in darkness for at least 30 minutes before fluorescence measurement. Minimal ( $F_0$ ) and maximal ( $F_m$ ) fluorescence yields were measured using dark-adapted leaves. The same parameters ( $F$ ) and ( $F_m'$ ) were measured upon light applications ( $150$  and  $500 \mu\text{mol m}^{-2} \text{s}^{-1}$ ). The radiation was maintained until both,  $F$  and  $F_m'$  were stable. The unit  $\mu\text{mol m}^{-2} \text{s}^{-1}$  corresponds to the photosynthetically active photon flux density (PPFD) or, by some scientists preferred term, photon irradiance equivalent to PPFD. Relative electron transport rate was calculated according to Schreiber *et al.*<sup>12</sup> For rel. ETR the unit  $\mu\text{mol m}^{-2} \text{s}^{-1}$  should be used.

Oxygen evolution was measured using the gas-phase Clark-type oxygen electrode (Hansatech). The leaf discs ( $2.5 \text{ cm}^2$ ) were placed in the reaction chamber and the oxygen evolution was measured in the dark and at two different light amounts applied (PPFD of  $150$  and  $500 \mu\text{mol m}^{-2} \text{s}^{-1}$ , respectively). The temperature inside the reaction chamber was  $25 \text{ }^\circ\text{C}$ .

### SDS-PAGE and Rubisco LSU Immunodetection

Plant material was powdered in liquid nitrogen and extracted with hot ( $80 \text{ }^\circ\text{C}$ ) buffer containing  $0.13 \text{ mol dm}^{-3}$  Tris-HCl ( $\text{pH} = 6.8$ ), 16 % (vol. fraction,  $\varphi$ ) glycerol,  $4.6 \text{ g} / 100 \text{ ml}$  SDS and  $0.59 \text{ g} / 100 \text{ ml}$  DTT. Proteins were determined according to Bradford,<sup>13</sup> using the bovine serum albumin (BSA) as a standard. Aliquots of each homogenate were mixed with corresponding volumes of denaturing  $0.065 \text{ mol dm}^{-3}$  Tris-HCl buffer containing  $6 \text{ g} / 100 \text{ ml}$  SDS, 6 % ( $\varphi$ )  $\beta$ -mercaptoethanol, 30 % ( $\varphi$ ) glycerol and  $0.01 \text{ g} / 100 \text{ ml}$  of bromphenol blue.<sup>14</sup> The extracts were boiled for 2 min. Constant protein mass ( $30 \mu\text{g}$  of total protein per lane) were analysed by SDS-PAGE (Mini Trans-Blot cell, Biorad) and subsequent Western blotting according to Towbin *et al.*<sup>15</sup> The resolving gel was made at 10 % (T) of polyacrylamide. Standard prestained proteins (Biorad) of known molecular weights were run in the same gel. The membranes were blocked with 10 % non-fat powdered milk solution made in PBS buffer ( $58 \text{ mmol dm}^{-3} \text{ Na}_2\text{HPO}_4$ ,  $17 \text{ mmol dm}^{-3} \text{ NaH}_2\text{PO}_4$ ,  $68 \text{ mmol dm}^{-3} \text{ NaCl}$ )  $\text{pH} = 7.4$  containing 1 % ( $\varphi$ ) of Tween 20 (TPBS buffer). The membrane was incubated with a rabbit monoclonal antibody raised against the pea Rubisco LSU (in a dilution of 1:1000 in TPBS buffer). The incubation was made overnight at  $4 \text{ }^\circ\text{C}$ . The membrane was washed for 20 min three times with TPBS buffer. The secondary antibody was an alkaline phosphatase-anti-rabbit IgG (Sigma) diluted 1:2000. The membrane was developed with BCIP/NBT (5-bromo-4-chloro-3-indolyl phosphate and nitroblue tetrazolium).

### DNA Analysis

Frozen leaf tissue (0.5 g) was grinded to a powder in liquid nitrogen. Total nucleic acids (TNA) were isolated according to Daire *et al.*<sup>16,17</sup> and Šeruga *et al.*<sup>18</sup> TNA (50 ng) isolated from green leaves was used to amplify PCR fragment of 199 bp, using primers: 5'-acatggacagctgtgtgac-3', 5'-gcaggccttaaacccaat-3'. Primers were designed on the

basis of *Acer rubrum* cultivar Florida Flame ribulose-1,5-bisphosphate carboxylase/oxygenase large subunit (rbcL) gene (DQ915972). PCR conditions were as follows: 5 min denaturation at 94 °C, 35 cycles (30 s 94 °C; 1 min 51 °C; 30 s 72 °C), 30 s 72 °C. Reaction was performed in a total volume of 50  $\mu\text{l}$  containing 5  $\mu\text{l}$  of 10 times diluted PCR buffer, 200  $\mu\text{mol dm}^{-3}$  of each dNTP, 0.625 U of AmpliTaq polymerase (AppliedBiosystems) and 0.2  $\mu\text{mol dm}^{-3}$  of each primer (U: one unit is defined as the amount of enzyme required to catalyzed the incorporation of 10  $\mu\text{mol}$  of dNTP into acid insoluble material in 30 min at 74 °C). Purification of the PCR product was done using Qiaquick PCR purification kit (Quiagen), according to the procedure proposed by manufacturer. Amplified fragment was labeled using Dig DNA labeling and detection kit (Roche). For dot blot, TNA from green (G), yellow green (YG) and yellow (Y) leaves was isolated as mentioned above. RNA was digested with RNase, according to the procedure proposed by manufacturer (Promega) and 2  $\mu\text{g}$  of each DNA sample were applied to a positively charged nylon membrane (Roche) and hybridized with 20 ng/ml of labeled probe at 45 °C, according to the procedure proposed by manufacturer (Roche). Plasmid ptz57 R/T DNA (200 ng) was included in the experiment as a negative control.

#### *Preparation of Extracts for Estimation of Lipid Peroxidation, Oxidatively Modified Proteins and SOD Activity*

Frozen leaf samples (0.2 g) were ground to a fine powder with liquid nitrogen and extracted with ice-cold 100  $\text{mmol dm}^{-3}$  potassium phosphate ( $\text{KPO}_4$ ) buffer (pH = 7) including 1  $\text{mmol dm}^{-3}$  EDTA, using pre-chilled mortars and pestles. The extracts were centrifuged at 18 000 g for 10 min at 4 °C. Before determination the extracts were re-centrifuged at 25 000 g for 20 min at 4 °C and resulting supernatants used for determination of SOD activity, thiobarbituric acid reactive substances (TBARS) and carbonyl group contents. Total soluble protein contents of the enzyme extracts were estimated according to Bradford<sup>13</sup> using bovine albumin serum (BSA, Sigma) as standard.

#### *Superoxide Dismutase Assay*

The activity of superoxide dismutase (SOD; 1.15.1.1) was assayed by measuring its ability to inhibit the photochemical reduction of nitroblue tetrazolium (NBT) following the method of Beauchamp and Fridovich.<sup>19</sup> The reaction mixture (3 ml) contained 50  $\text{mmol dm}^{-3}$   $\text{KPO}_4$  buffer (pH = 7.8), 13  $\text{mmol dm}^{-3}$  methionine, 75  $\mu\text{mol dm}^{-3}$  NBT, 2  $\mu\text{mol dm}^{-3}$  riboflavin, 0.1  $\text{mmol dm}^{-3}$  EDTA and 0.1 ml of enzyme solution. The enzyme solution was prepared by dilution of the enzyme extract with the protein extraction buffer, so that 0.1 ml of the enzyme solution corresponds to 2.5, 5.0, 7.5 or 10.0  $\mu\text{l}$  of the original enzyme extract. Riboflavin was added at the end and the test tubes were shaken and placed below light source (two 15 W fluorescent lamps). The reaction was allowed to go for 10 min and was stopped by switching off the light. The absorbance of the solution was

measured at 560 nm. The non irradiated reaction mixture served as control and was deducted from  $A_{560}$ . The reaction mixture lacking the enzyme developed the most color and this decreased with increasing volume of extract added.  $A_{560}$  was plotted as a function of the volume of enzyme extract in the reaction mixture. From the resultant graph the volume of the enzyme extract corresponding to 50 % inhibition of the reaction was read and considered as one enzyme unit (U).

#### *Lipid Peroxidation and Carbonyl Content*

Lipid peroxidation was determined by estimating the amount of TBARS using the thiobarbituric acid method described by Heath and Packer.<sup>20</sup> The crude extracts were mixed with 0.25 g / 100 ml thiobarbituric acid solution containing 10 g / 100 ml trichloroacetic acid, heated at 95 °C for 30 min and the reaction was stopped in an ice bath. The cooled mixtures were centrifuged at 10 000 g for 10 min and the MDA content calculated from the absorbance at 532 nm (correction was done by subtracting the absorbance at 600 nm for non-specific turbidity) by using extinction coefficient of 155  $\text{dm}^3 \text{mmol}^{-1} \text{cm}^{-1}$ .

Oxidative damage to proteins was estimated as the content of carbonyl group.<sup>21</sup> The carbonyl groups in the protein side chain were derivatized to 2,4-dinitrophenylhydrazone by reaction with 2,4-dinitrophenylhydrazine (DNPH) dissolved in HCl, accompanied by HCl blanks alone. After the DNPH reaction, the samples were kept in dark for 1 hour and mixed every 15 min. Proteins were precipitated with an equal volume of 10 g / 100 ml TCA, centrifuged at 12 000 g for 10 min and the pellets were washed three times with 0.5 ml of ethanol + ethyl acetate mixture (1:1). Finally, the precipitates were dissolved in (6 M urea + HCl) solution and the absorbance peak at 370 nm was determined spectrophotometrically. Protein contents were determined on the HCl-blank pellets using a bovine albumin serum (BSA) standard curve in urea + HCl and reading the absorbance at 280 nm.

#### *Data Analysis*

Data were analyzed by one-way analysis of variance (ANOVA) with 5 replicates from every leaf type. The mean values were compared using LSD test. Differences were considered significant at  $P \leq 0.05$ . All statistical analyses were done with Statistica 7.1. software (StatSoft, Inc. 2005).

## RESULTS AND DISCUSSION

Decrease in photosynthetic activity and degradation of chlorophyll is a hallmark of leaf senescence process.<sup>3</sup> Content of total chlorophylls (Chl *a+b*), maximum quantum yield of PSII ( $F_v/F_m$  value; the ratio of variable and maximal fluorescence) and relative electron transport rate (rel. ETR) in green (G), yellow-green (YG) and yellow (Y) maple leaves are shown in Figure 1. Values for total chlorophylls content were 1.83 (100 %), 0.55 (30 %) and 0.15 (8 %) mg/g of fresh leaves in G, YG and Y leaves,

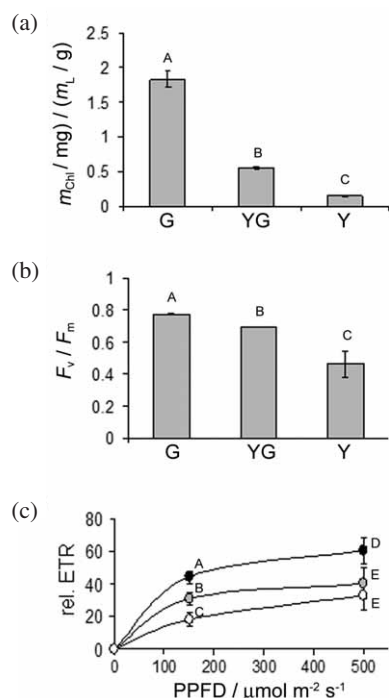


Figure 1. Total chlorophylls content (a), maximum quantum yield of PSII ( $F_v/F_m$ ) (b) and relative electron transport rate (rel. ETR) (c) in green (G; black circles), yellow-green (YG; grey circles) and yellow (Y; white circles) leaves of maple (*Acer pseudoplatanus* L.). Significant differences between G, YG and Y leaves were designated by different letters (A, B, C, D and E) placed on the top of the column (a and b) or near the circles (c). Symbols:  $m_{chl}$  – mass of total chlorophylls;  $m_L$  – mass of fresh leaves; PPFD – photosynthetically active photon flux density.

respectively (Figure 1a). Such significant decrease of chlorophylls content reflected on maximum quantum yield of PSII (Figure 1b), as seen as decrease in  $F_v/F_m$  value from 0.774 (100 %) in G leaves to 0.694 (90 %) and 0.465 (60 %) in YG and Y ones, respectively. However, decline in  $F_v/F_m$  was not equally fast as total chlorophylls degradation. Lu and Zhang<sup>22</sup> revealed considerable decrease in total chlorophylls content (64 %) accompanied with small (4 %) but significant decrease in  $F_v/F_m$  value in senescent maize (*Zea mays* L. cv. Yedan 13) leaves. Decrease in chlorophyll level accompanied with retained high  $F_v/F_m$  values in senescent rice (*Oryza sativa* L.) leaves was also reported by Tang *et al.*<sup>23</sup> In spite of  $F_v/F_m$  decrease, the changes of non photochemical quenching of chlorophyll fluorescence (NPQ) values in senescent leaves appeared not to be statistically significant at low light level applied (PPFD = 150  $\mu\text{mol m}^{-2} \text{s}^{-1}$ : 0.54  $\pm$  0.27, 0.71  $\pm$  0.18 and 0.66  $\pm$  0.19 in G, YG and Y leaves, respectively) as well as at moderate light level applied (PPFD = 500  $\mu\text{mol m}^{-2} \text{s}^{-1}$ : 1.99  $\pm$  0.60, 1.85  $\pm$  0.60 and 1.44  $\pm$  0.18 in G, YG and Y leaves, respectively). This would ensure efficient protection of PSII protein components (e.g. D1 protein) against destruction by excess excitation energy and enable its extended relatively high maximum

photochemical efficiency ( $F_v/F_m$ ) during leaf senescence. PSII driven relative electron transport rate (rel. ETR) was significantly decreased in YG and Y leaves when compared to G leaves (Figure 1c). This could be due to changed heterogeneity of PSII reaction centers in senescent leaves, which would inhibit the reducing activity of PSII at the level of plastoquinone ( $Q_A$ ).<sup>22</sup> Since the clear relationship between photosynthetic electron transport and  $\text{CO}_2$  fixation was established<sup>24</sup> it was also likely that lower demands for ATP and NADPH due to decreased  $\text{CO}_2$  fixation in senescent leaves would down regulate rel. ETR.<sup>22</sup> As reviewed by Krupinska and Humbeck<sup>25</sup> the major factor responsible for reduced photosynthetic capacity during senescence is decline in Rubisco content. It appeared that small Rubisco subunit (SSU) was more stable than the large one (LSU) during natural senescence of barley (*Hordeum vulgare* L. cv. Carina).<sup>26</sup> We investigated the appearance of 55 kDa polypeptide on SDS polyacrylamide gel (Figure 2a) which was further confirmed to react with antibody raised against LSU (Figure 2b). The loss of 55 kDa polypeptide as well the LSU band on immunoblot was demonstrated (Figure 2). Decrease in Rubisco abundance during senescence was shown to arise as a consequence of both, its degradation as well as its reduced biosynthesis.<sup>27</sup> Our results also demonstrate the degradation of *rbcL* gene during the senescence of *Acer pseudoplatanus* L. Dot blot results (Figure 2c) demonstrated the decrease of hybridization intensity in YG and Y leaves compared to green ones. This revealed that with the senescence, the portion of *rbcL* in the overall amount of DNA was rapidly decreasing. Such reduced template availability would imply its decreased transcriptional capability and consequently reduced biosynthesis of Rubisco LSU. However, the LSU level was not enti-

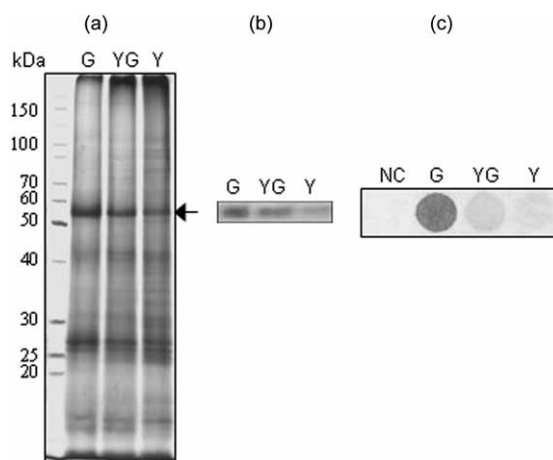


Figure 2. Rubisco LSU protein and *rbcL* gene abundance in green (G), yellow-green (YG) and yellow (Y) leaves of maple (*Acer pseudoplatanus* L.). (a) SDS-PAGE profile of soluble and membrane proteins (the 55 kDa polypeptide that represent Rubisco LSU is indicated by arrow). (b) Immunoblot analysis of Rubisco LSU. (c) Dot blot analysis of *rbcL* gene; NC – negative control (Plasmid ptz57 R/T DNA).



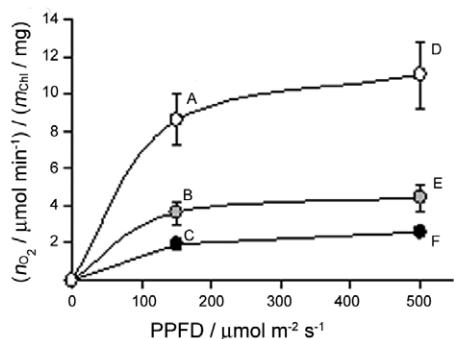


Figure 3. The capacity of PSII for oxygen evolution in green (G; black circles), yellow-green (YG; grey circles) and yellow (Y; white circles) leaves of maple (*Acer pseudoplatanus* L.). Significant differences between G, YG and Y leaves were designated by different letters (A, B and C at PPFD of  $150 \mu\text{mol m}^{-2} \text{s}^{-1}$  as well as D, E and F at  $500 \mu\text{mol m}^{-2} \text{s}^{-1}$ ) placed near the circles. Symbols:  $n_{\text{O}_2}$  – oxygen amount;  $m_{\text{ChI}}$  – mass of total chlorophylls; PPFD – photosynthetically active photon flux density.

rely correlated with *rbcL* levels seen on dot blots. Degradation of *rbcL* was more pronounced than LSU protein, especially in YG leaves. The negative DNA control (plasmid which did not contain *rbcL*) showed no measurable signal of hybridization (Figure 2c). Decline in Rubisco LSU reflects to its overall activity and thus to  $\text{CO}_2$  fixation<sup>2</sup> which was prerequisite for down regulation of photosynthetic electron transport rate (Figure 1c).

Although the capacity of PSII for oxygen evolution decreased in senescent maple leaves when expressed per leaf area or fresh weight (data not shown), its significant increase was recorded when expressed per chlorophyll unit (Figure 3). Yellow leaves produced about 4.5 and 2.5 times more oxygen than G and YG leaves, respectively. So, the yellow leaves appeared to have the highest oxygen production per chlorophyll unit and the lowest relative electron transport rate at the same time. According to some information, the rate of  $\text{CO}_2$  fixation is high enough to convert about up to 50 % of total excitation energy,<sup>3</sup> while the rest is directed to alternative electron acceptors like molecular oxygen. As the consequence, superoxide ( $\text{O}_2^{\cdot-}$ ) and singlet oxygen ( $^1\text{O}_2$ ) are formed.<sup>8,9</sup> The increase in ROS level during natural senescence in some species was shown to be associated with increased level of lipid peroxidation, carbonyl content and superoxide dismutase activity.<sup>28,29</sup> The level of SOD activity in our investigation was not significantly changed in YG leaves, but increased 3.5-fold in Y leaves (344 %) (Figure 4). The oxidative damage to lipids and proteins, measured as TBARS and carbonyl content also increased during maple leaf yellowing (Figure 5). Lipid peroxidation increased continuously during senescence (Figure 5a). YG and Y leaves had TBARS level about 160 and 180 %, respectively, of that in G leaves. The level of carbonyl content revealed, however, identical dynamics as SOD activity – the significant increase occurred only in Y lea-

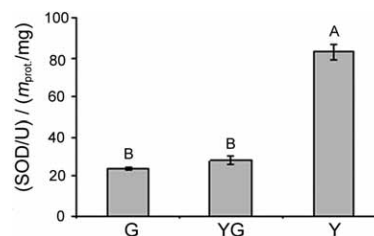


Figure 4. The activity of superoxide dismutase (SOD) in green (G), yellow-green (YG) and yellow (Y) leaves of maple (*Acer pseudoplatanus* L.). Significant differences between G, YG and Y leaves were designated by different letters (A and B) placed on the top of the column. Symbols and units:  $m_{\text{prot.}}$  – mass of protein; U – one SOD unit corresponds to the volume of enzyme extract that inhibits the photochemical reaction of NBT for 50 %.

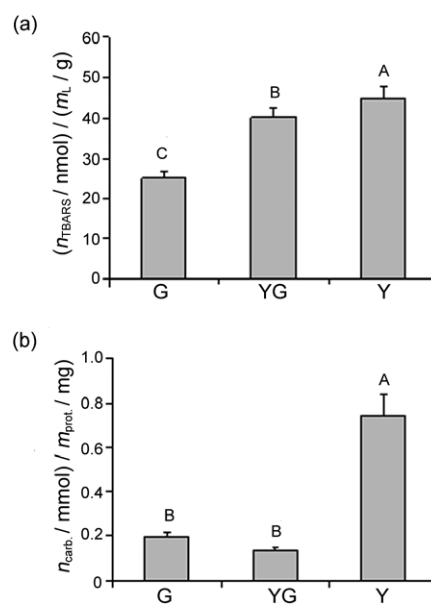


Figure 5. Changes in oxidative stress parameters in green (G), yellow-green (YG) and yellow (Y) leaves of maple (*Acer pseudoplatanus* L.). (a) Lipid peroxidation (expressed as TBARS amount per mass of fresh leaves). (b) Protein oxidation (defined as the amount of carbonyl groups per mass of protein). Significant differences between G, YG and Y leaves were designated by different letters (A, B and C) placed on the top of the column. Symbols:  $n_{\text{TBARS}}$  – TBARS amount;  $m_L$  – mass of fresh leaves;  $n_{\text{carb.}}$  – amount of carbonyl groups;  $m_{\text{prot.}}$  – mass of protein.

ves which showed 3.8 and 5.5 times higher values than G and YG leaves, respectively (Figure 5b). Such differential dynamics of oxidative damage to lipids and proteins raised the question on its sensitivity to particular ROS. Since the highest increase in TBARS level was measured in YG leaves it can be speculated that this was due to potential superoxide radical and singlet oxygen increase. Considerable increase in SOD activity in Y leaves (Figure 4) should converse certain amount of superoxide to hydrogen peroxide. Since the increase in SOD activity corroborated with significant increase of carbonyl content it can be further speculated that oxidative damage to

proteins was due to potential increase in H<sub>2</sub>O<sub>2</sub> level. Indeed, the study of oxidative stress on isolated chloroplasts done by Desimone *et al.*<sup>30</sup> revealed that H<sub>2</sub>O<sub>2</sub>, but not the superoxide radical, was directly involved in degradation of Rubisco LSU.

Based on the presented results it can be concluded that besides chlorophyll degradation, natural senescence of maple leaves was characterized by down regulation of photosynthetic electron transport and degradation of Rubisco LSU. This was not, however, accompanied with equally fast decline in PSII capacity for oxygen production leading to oxidative stress. Enhanced production of ROS was manifested as increased content of TBARS and protein carbonyls. Also, considerable increase in SOD activity in later phase of senescence was observed. This probably influenced the superoxide to hydrogen peroxide ratio and accordingly to regulated protein degradation as well as triggered programmed cell death (PCD). Nevertheless, in order to obtain a complete picture of physiological events which take place during natural senescence, it remains to investigate other antioxidative enzymes and changes in hydrogen peroxide level.

## REFERENCES

1. L. D. Noodén, J. J. Guiamét, and I. John, *Physiol. Plant.* **101** (1997) 746–753.
2. C. Smart, *New Phytol.* **126** (1994) 419–448.
3. P. Zimmermann and U. Zentgraf, *Cell. Mol. Biol. Lett.* **10** (2005) 515–534.
4. J. F. Dat, S. Vandenamee, E. Vranová, M. Van Montagu, D. Inzé, and F. Van Breusegem, *Cell. Mol. Life Sci.* **57** (2000) 779–795.
5. S. J. Neill, R. Desikan, and J. T. Hancock, *Curr. Opin. Plant Biol.* **5** (2002) 388–395.
6. R. Mittler, *Trends Plant Sci.* **7** (2002) 405–410.
7. R.G. Alscher, J. L. Donahue, and C. L. Cramer, *Physiol. Plant.* **100** (1997) 224–233.
8. A. Arora, R. K. Sairam, and G. C. Srivastava, *Curr. Sci.* **82** (2002) 1227–1238.
9. S. Hippeli, I. Heiser, and E. F. Elstner, *Plant Physiol. Biochem.* **37** (1999) 167–178.
10. E. Beers, *Cell Death Differ.* **4** (1997) 649–661.
11. H. K. Lichtenthaler, *Methods Enzymol.* **148** (1987) 350–382.
12. U. Schreiber, W. Bilger, and C. Neubauer, *Ecol. Stud.* **100** (1994) 49–70.
13. M. M. Bradford, *Anal. Biochem.* **72** (1976) 248–254.
14. U. K. Laemli, *Nature* **227** (1970) 680–685.
15. H. Towbin, T. Staehelin, and J. Gordon, *Proc. Natl. Acad. Sci. USA.* **76** (1979) 4350–4354.
16. X. Daire, E. Boudon-Padieu, A. Berville, B. Schneider, and A. Caudwell, *Ann. Appl. Biol.* **121** (1992) 95–103.
17. X. Daire, D. Clair, W. Reinert, and E. Boudon-Padieu, *Eur. J. Plant Pathol.* **103** (1997) 507–514.
18. M. Šeruga, D. Škorić, S. Botti, S. Paltrinieri, N. Juretić, and A. F. Bertaccini, *Forest Pathol.* **33** (2003) 113–125.
19. C. Beauchamp and I. Fridovich, *Anal. Biochem.* **44** (1971) 276–287.
20. R. L. Heath and L. Packer, *Arch. Biochem. Biophys.* **125** (1968) 189–198.
21. R. L. Levine, J. A. Williams, E. A. Stadtman, and E. Shacter, *Methods Enzymol.* **233** (1994) 346–357.
22. C. Lu and J. Zhang, *J. Exp. Bot.* **49** (1998) 1671–1679.
23. Y. Tang, X. Wen and C. Lu, *Plant Physiol. Biochem.* **43** (2005) 193–201.
24. J. P. Krall and G. E. Edwards, *Physiol. Plant.* **86** (1992) 180–187.
25. K. Krupinska and K. Humbeck, *Photosynthesis and chlorophyll breakdown* in: L. D. Noodén (Ed.), *Plant Cell Death Processes*, Elsevier Academic Press, San Diego, 2004, pp. 169–187.
26. K. Humbeck and K. Krupinska, *J. Photochem. Photobiol.* **36** (1996) 321–326.
27. T. Mae, *Leaf senescence and nitrogen metabolism*, in: L. D. Noodén (Ed.), *Plant Cell Death Processes*, Elsevier Academic Press, San Diego, 2004, pp. 157–168.
28. G. M. Pastori and L. A. del Rio, *Plant Physiol.* **113** (1997) 411–418.
29. M. J. Hernandez-Jimenez, M. M. Lucas, and M. R. de Felipe, *Plant Physiol. Biochem.* **40** (2002) 645–657.
30. M. Desimone, A. Henke, and E. Wagner, *Plant Physiol.* **111** (1996) 789–796.

## SAŽETAK

### Fotosintetski transport elektrona i aktivnost superoksid-dismutaze tijekom prirodne senescencije listova javora

Hrvoje Lepeduš, Ivna Štolfa, Sandra Radić, Mirna Ćurković Perica, Branka Pevalek-Kozlina i Vera Cesar

U ovom istraživanju proučena je prirodna senescencija listova javora (*Acer pseudoplatanus* L.). Proučavana su tri tipa senescentnih listova: zeleni, žutozeleni i žuti. Uslijed značajne razgradnje ukupnih klorofila, sniženja maksimalnog prinosa fotosustava II ( $F_v/F_m$ ) i sniženja relativne stope transporta elektrona (rel. ETR, engl. *relative electron transport rate*) došlo je do smanjenja učinkovitosti fotosinteze. Također, u žutim i žutozelenim

listovima snižen je sadržaj Rubisco LSU-a, te je uočena degradacija gena *rbcL*. Sposobnost fotosustava II za produkciju kisika, izražena po jedinici klorofila, značajno je porasla u senescentnim listovima, što je najvjerojatnije bilo izvorom suviška reaktivnih kisikovih jedinki (ROS, engl. *reactive oxygen species*). Aktivnost superoksid dismutaze (SOD, engl. *superoxide dismutase*) porasla je 3.5 puta u žutim listovima, u odnosu na zelene i žutozelene. Povećanje razine ROS-a, kao i aktivnosti SOD-a, tijekom prirodne senescencije listova javora bilo je povezano s povećanom razinom lipidne peroksidacije i sadržaja karbonila u proteinima.